

## MIT Open Access Articles

*Seasonal Loops Between Local Outgoing  
Longwave Radiation and Surface Temperature*

The MIT Faculty has made this article openly available. **Please share** how this access benefits you. Your story matters.

**Citation:** Richards, B. D. G., Koll, D. D. B., & Cronin, T. W. (2021). Seasonal loops between local outgoing longwave radiation and surface temperature. *Geophysical Research Letters*, 48, e2021GL092978.

**As Published:** <http://dx.doi.org/10.1029/2021gl092978>

**Publisher:** American Geophysical Union (AGU)

**Persistent URL:** <https://hdl.handle.net/1721.1/140401>

**Version:** Author's final manuscript: final author's manuscript post peer review, without publisher's formatting or copy editing

**Terms of use:** Creative Commons Attribution-Noncommercial-Share Alike



# Seasonal Loops between Local Outgoing Longwave Radiation and Surface Temperature

Benjamin D.G. Richards<sup>1,2</sup>, Daniel D.B. Koll<sup>3</sup>, Timothy W. Cronin<sup>2</sup>

<sup>1</sup>Department of Physics; Imperial College London

<sup>2</sup>Department of Earth, Atmospheric and Planetary Sciences; MIT

<sup>3</sup>Department of Atmospheric and Oceanic Sciences; Peking University

## Key Points:

- Monthly outgoing longwave radiation (OLR) is a multivalued function of local surface temperature, exhibiting loops and other complex shapes.
- OLR loops occur both in clear-sky and all-sky data, so the behavior is robust to clouds.
- OLR loops arise because humidity lags surface temperature in the tropics, and lapse rates lead surface temperature in the extratropics.

---

Corresponding author: Benjamin Richards, [b.d.g.richards@gmail.com](mailto:b.d.g.richards@gmail.com)

This is the author manuscript accepted for publication and has undergone full peer review but has not been through the copyediting, typesetting, pagination and proofreading process, which may lead to differences between this version and the [Version of Record](#). Please cite this article as [doi: 10.1029/2021GL092978](https://doi.org/10.1029/2021GL092978).

This article is protected by copyright. All rights reserved.

Author Manuscript

**Abstract**

The relationship between outgoing longwave radiation (OLR) and surface temperature has a major influence on Earth’s climate sensitivity. Studies often assume that this relationship is approximately linear, but it is unclear whether the approximation always holds. Here we show that, on seasonal timescales, clear-sky OLR is a multivalued function of local surface temperature. In many places the OLR-temperature relationship is better approximated by a loop than a line and we quantify the resulting “OLR loopiness”, that is, how much clear-sky OLR varies between different seasons with the same surface temperature. Based on offline radiative calculations, in the tropics OLR loops are mainly caused by seasonal variations in relative humidity that are out of phase with surface temperature; in the extratropics OLR loops are mainly due to variations in lapse rates. Our work provides a mechanism through which Earth’s climate feedback can differ between seasonal and long-term time scales.

**Plain Language Summary**

When the Earth is warmer, it loses more heat to space. The simplest formula describing this relationship is a line with an upwards slope, where the slope determines how much Earth warms from added greenhouse gases. Here we report that the relationship between local temperature and rate of heat loss to space can be more complicated on seasonal time scales, often taking the form of loops or other curved shapes. We come up with a way to measure how big these loops are, and explain why they happen. Our results underline that Earth’s response to seasonal changes is generally different from Earth’s response to global warming.

**1 Introduction**

The long-term relationship between surface temperature and OLR has a major influence on Earth’s climate sensitivity, or how much global temperature will respond to a given global energy imbalance (e.g., Zelinka et al., 2020). One way to constrain this relationship is to draw on measurements of Earth’s radiative budget on timescales that are short enough to be easily observed, such as interannual and seasonal variability. Pioneering work in this area found that the relation between surface temperature and OLR was nearly linear, with a slope  $d\text{OLR}/dT_s \sim 2 \text{ W m}^{-2} \text{ K}^{-1}$  (Budyko, 1969). The basic assumption of a linear relationship has remained in wide use since then, as underlined by the common use of linear regression in empirical studies of Earth’s climate sensitivity (e.g., Forster & Gregory, 2006; Murphy et al., 2009; Dessler, 2010; Forster, 2016). The goal of this paper is to revisit when the assumption of a linear relationship between OLR and surface temperature breaks down.

On long time scales, theoretical reasoning and climate models both suggest that a linear relationship is a valid assumption (Koll & Cronin, 2018; Zhang et al., 2020). Extrapolating to shorter time scales, one would therefore expect that the seasonal cycle of OLR at a given location also traces out a line, increasing as the surface warms and decreasing as it cools.

Figure 1 shows the coefficient of determination  $R^2$  for a linear fit between climatological monthly clear-sky OLR from CERES and surface temperature  $T_s$  data from ERA5 (our detailed methods are described in Section 2). A linear OLR- $T_s$  relationship appears adequate in parts of the world where seasonal surface temperature variations are large, particularly over extratropical continents.

Many locations, however, show only a weak linear correlation between monthly  $T_s$  and OLR, and the spread of best-fit slopes is much broader in the tropics than in the extratropics. These patterns have been discussed before; for example, Raval et al. (1994) showed that relative humidity controls local OLR more strongly than does surface temperature in the tropics, while Allan et al. (1999) and Huang and Ramaswamy (2008) explored how covariance between relative humidity and surface temperature can lead to a “super-greenhouse effect” where many regions in the tropics show a decrease in local OLR with increasing  $T_s$  on seasonal and interannual time scales.

**Figure 1.** On seasonal time scales, the relation between clear-sky OLR and surface temperature can deviate strongly from linearity. (a) Coefficient of determination ( $R^2$ ) for a linear fit of monthly local clear-sky OLR against local surface temperature. (b) Histogram of best-fit slopes of OLR against  $T_s$  in different regions; the area-weighted global mean of local slopes is  $0.99 \text{ W m}^{-2} \text{ K}^{-1}$ .

**Figure 2.** The relation between clear-sky OLR and surface temperature  $T_s$  is approximately linear at a global scale, yet it arises from far more complex relations locally. (a-e) In many locations these relations take the form of OLR-surface temperature loops. The locations correspond to the labels in Figure 1a, arrows indicate the seasonal progression. (f) The global relationship between OLR and surface temperature (grey), with local loops from panels a-e imposed on top.

What form does the relationship between OLR and surface temperature take in regions where the linear correlation between the two is weak?

Figure 2 shows the climatological annual cycles of monthly clear-sky OLR and surface temperature  $T_s$  data at select locations noted as a through e on Figure 1 (to view other locations, see [bdgrichards.github.io/OLR-Loop-Viewer](https://github.com/bdgrichards/OLR-Loop-Viewer) and zoom in). It is clear that the cycles are far from random; instead they often trace loops or more complex curves. These loops appear prominently in the tropics, but also show up over many midlatitude and subpolar ocean regions (e.g., Figure 2b), embedded in an overall envelope of monthly  $\text{OLR}(T_s)$  values that is mostly linear (Figure 2f). Loops, rather than lines or nonlinear but still single-valued curves such as parabolas, imply that the same surface temperature is associated with different values of OLR at different points in the seasonal cycle.

How can non-uniqueness arise in the monthly  $\text{OLR}(T_s)$  relationship? Since the dominant controls on clear-sky OLR on a seasonal time scale are surface temperature  $T_s$ , the atmospheric temperature profile, and the atmospheric relative humidity profile, we can reason that a non-unique clear-sky  $\text{OLR}(T_s)$  must arise from a seasonal cycle of atmospheric temperature or relative humidity that is out of phase with surface temperature.

We refer to such a non-unique relationship between OLR and surface temperature as OLR loops. In the rest of this paper we describe the spatial pattern of seasonal OLR loops and explain the mechanisms that give rise to them. For simplicity we focus on clear-sky OLR; clouds are neglected aside from a brief discussion in Section 4. We first introduce a metric for the magnitude and directionality of OLR loops, which points to a pronounced contrast between the tropics and extratropics. We then use a radiative transfer model, and find that tropical OLR loops are primarily due to relative humidity variations that are out of phase with surface temperature, whereas extratropical OLR loops are primarily due to lapse rate variations that are out of phase with surface temperature. We conclude by briefly discussing some tentative implications of OLR loops for attempts to constrain Earth’s long-term climate sensitivity via short-term observations.

## 2 Methods

We use surface temperatures from ERA5 reanalysis data and satellite-based OLR values from CERES (Hersbach et al., 2020; Loeb et al., 2018). Variables are monthly means spanning the years 2001 to 2020, with a horizontal resolution of  $1^\circ \times 1^\circ$ . Surface temperature is taken as the air temperature at 2m above the surface. To quantify the typical seasonal difference in clear-sky OLR at a given location, as illustrated by the curves in Figure 2a-e, we define the “loopiness” metric  $\mathcal{O}$  as

$$\mathcal{O} = \frac{1}{\Delta T_s} \int \text{OLR} dT_s. \quad (1)$$

**Figure 3.** (a) Map of OLR “loopiness”  $\mathcal{O}$  based on ERA5 and CERES data. Loopiness quantifies the typical seasonal OLR difference at a fixed surface temperature, with positive values corresponding to a clockwise OLR-surface temperature loop; see text. (b,c) Our offline OLR calculations recover the observed mean OLRs as well as observed OLR loopiness values. The mean absolute error in panel (b) is  $5.21 \text{ W m}^{-2}$ , the mean absolute error in panel (c) is  $1.78 \text{ W m}^{-2}$ . The color scale in (b,c) corresponds to the number of lat/lon/time points within a given OLR bin – note the log axis.

Here  $\Delta T_s$  is the annual range in surface temperature computed as the difference in temperature between the warmest and coolest month. We use long-term monthly means, so the vertices of the loop correspond to the climatological  $T_s$  and OLR for each calendar month. The sign of  $\mathcal{O}$  defines a loop’s direction: loops with positive area are clockwise (OLR leads  $T_s$ ), and loops with negative area are counterclockwise (OLR lags  $T_s$ ). In situations where the curve of OLR versus surface temperature intersects itself (e.g., Figure 2c), the sign of  $\mathcal{O}$  measures the average direction. The integrals have units of  $\text{W/m}^2 \times \text{K}$ , so  $\mathcal{O}$  is defined in  $\text{W/m}^2$ . When there is a single loop,  $\mathcal{O}$  represents the typical OLR difference between two parts of the seasonal cycle that have the same surface temperature.

To interpret the observed pattern of OLR loopiness we also perform offline radiative calculations, using the Rapid Radiative Transfer Model for Global Climate Models (RRTMG; Mlawer et al., 1997) and the CLIMLAB python package (Rose, 2018). In addition to ERA5 surface temperatures, the calculations use ERA5 atmospheric temperatures and relative humidities, as well as a climatological ozone profile.

We validate our offline radiative calculations by using RRTMG with ERA5 atmosphere and surface data to reproduce the clear-sky OLRs from CERES. Our calculations closely match the CERES clear-sky OLR values, with a mean absolute error of  $5.21 \text{ W m}^{-2}$  (Figure 3b). Our offline calculations also broadly reproduce  $\mathcal{O}$ , with a mean absolute error of  $1.78 \text{ W m}^{-2}$  and a bias of  $1.17 \text{ W m}^{-2}$  (Figure 3c). As we show below, the magnitude of  $\mathcal{O}$  ranges from several  $\text{W m}^{-2}$  up to  $19 \text{ W m}^{-2}$ , so we consider an error of  $\sim 2 \text{ W m}^{-2}$  in our offline calculations sufficiently accurate.

### 3 Global Map of OLR Loops

Figure 3a shows that the global map of OLR loopiness  $\mathcal{O}$  is dominated by three large-scale patterns. First, the magnitude of  $\mathcal{O}$ ,  $|\mathcal{O}|$ , is markedly higher in the tropics than in the extratropics. Second, in the extratropics  $|\mathcal{O}|$  is greater over oceans than over continents. Third, loops in the tropics also show a land-ocean contrast in which areas with strong negative loopiness tend to occur over tropical and subtropical ocean basins. A link to an interactive and more detailed version of Figure 3, which additionally allows users to zoom in on the underlying monthly  $T_s$ -OLR curve at each latitude-longitude point, can be found in the Acknowledgements.

The directionality of the OLR loops gives important information on what controls their global pattern. Loops are mostly clockwise, or positively oriented, across the globe, with the exception of some tropical ocean regions and Antarctica (Figure 3). Positive loopiness means OLR leads  $T_s$ , or that for a given surface temperature, OLR is greater when the surface is warming than when the surface is cooling. Two end-member scenarios that can lead to positive loopiness are if (a) atmospheric temperatures  $\mathbf{T}_A$  lead surface temperatures while atmospheric humidity remains constant, or if (b) atmospheric relative humidity  $\mathbf{RH}$  lags surface temperatures while atmospheric and surface temperatures remain in phase. We use boldface for both the temperature and relative humidity profiles,  $\mathbf{T}_A$  and  $\mathbf{RH}$ , to indicate that they represent the full vertical structure of each quantity.

To attribute the OLR loops to variations in atmospheric temperature and humidity that are out of phase with  $T_s$ , we use offline calculations. The calculations compute OLR while

**Figure 4.** Illustration of our OLR loopiness decomposition. Left and middle columns show vertical temperature and relative humidity profiles, right column shows the resulting OLR- $T_s$  loops.

We compute monthly OLR for four different cases, where color saturation indicates different months (January = lightest shade, December = darkest shade). “Base case”: monthly  $T_s$ , annual-mean  $\mathbf{T}_A - T_s$  and  $\mathbf{RH}$  profiles; “Temperature Variation Only”: monthly  $\mathbf{T}_A - T_s$  and annual-mean  $\mathbf{RH}$  profiles; “Moisture Variation Only”: annual-mean  $\mathbf{T}_A - T_s$  and monthly  $\mathbf{RH}$  profiles; “Full Case”: monthly  $\mathbf{T}_A - T_s$  and  $\mathbf{RH}$  profiles. See text for more details. Profiles shown correspond to (32°N, 237°E), which is off the coast of California.

**Figure 5.** Attribution of OLR loopiness based on offline radiative calculations; compare to Fig. 3. (a) Only vertical temperature structure is allowed to vary seasonally. (b) Only moisture is allowed to vary seasonally.

holding the vertical temperature structure  $\mathbf{T}_A - T_s$  and/or the relative humidity profile  $\mathbf{RH}$  fixed. We use relative humidity instead of specific humidity to prevent unphysical conditions in the offline attribution. If one held specific humidity fixed while allowing temperature to vary seasonally, the atmospheric profiles would be strongly super-saturated in extratropical winter. The use of relative humidity as a state variable avoids this issue (Held & Shell, 2012).

The resulting four cases are illustrated in Figure 4. First, in the “base case,”  $T_s$  varies for each month while the lapse rate  $\mathbf{T}_A - T_s$  and relative humidity are fixed at their annual-mean values (Fig. 4, top). Because all atmospheric variables in the base case are in phase with surface temperature, there are no OLR loops. Second, in the “temperature variation” case we keep  $\mathbf{RH}$  fixed at its annual-mean profile but use full  $\mathbf{T}_A - T_s$  profiles from ERA5. In this case, all loops are due to lapse rate variations. Third, in the “moisture variation” case we use varying monthly profiles of  $\mathbf{RH}$  from ERA5 while keeping the lapse rate  $\mathbf{T}_A - T_s$  at its annual-mean value. In this case, all loops are due to humidity variations. Finally, in the “full case” described in Section 2, we use monthly ERA5 profiles for both  $\mathbf{RH}$  and  $\mathbf{T}_A - T_s$ . As a reminder, these calculations adequately reproduce both observed mean OLR and observed OLR loopiness from CERES.

We find that our offline calculations capture the dominant patterns of OLR loopiness. In the extratropics OLR loops primarily arise from lapse variations, while in the tropics OLR loops primarily arise from relative humidity variations (see Figure 5 versus Figure 3).

## 4 What causes OLR Loops

Comparing Figures 3 and 5 we can now interpret the mechanisms that give rise to OLR loops. First, loopiness over extratropical continents is small in both data and offline calculations, indicating that surface and atmosphere are largely in phase. The seasonal cycle over extratropical continents thus most closely resembles our “base case”. In contrast, loops are clockwise over extratropical oceans because of lapse rate variations (Fig. 5a). We attribute this to the large heat capacity of the ocean mixed layer, such that in spring the atmosphere tends to be warmer relative to the surface than it is in fall. OLR is thus higher when the surface is heating than when it is cooling, and  $\mathcal{O} > 0$  over extratropical oceans. The resulting loops also reduce the explanatory power of linear regression, particularly over the Southern Ocean, where  $R^2$  values are systematically lower than over extratropical continents (Fig. 1).

Second, in contrast to extratropical continents, loops over most tropical continents are clockwise because of humidity variations (Figs. 3 and 5b). These loops are consistent with the seasonal cycle in monsoon regions, in which surface temperature over land peaks early in the season and is followed by peaks in rainfall and humidity (e.g., Hartmann, 2016). If we consider the atmosphere before and after the surface temperature peak, OLR will be higher when the surface is heating up and the atmosphere is dry than when the surface is cooling

**Figure 6.** Normalized OLR loopiness,  $\mathcal{O}/\Delta\text{OLR}$ , where  $\Delta\text{OLR}$  is the local annual range of OLR, using (a) clear-sky data, and (b) all-sky data.

down and the atmosphere is humid. A clear example is the Indian subcontinent, but similarly large positive loopiness can also be seen in other monsoon regions such as South America, West Africa, and northern Australia.

Third, loops over tropical oceans arise from relative humidity variations (compare Fig. 3 and 5b), but their orientation can be either clockwise or counter-clockwise. For example, close to the coast of Namibia the seasonal cycle of atmospheric humidity leads surface temperatures, so  $\mathcal{O} < 0$ , whereas over the northern Indian Ocean humidity lags surface temperatures, so  $\mathcal{O} > 0$ . We attribute these patterns to the fact that tropical humidity is controlled by large-scale atmospheric dynamics (Pierrehumbert & Roca, 1998). In contrast, tropical SSTs are modulated by local insolation forcing as well as regional processes such as ocean upwelling (Schneider, 1996). The seasonal cycles of tropical SST and humidity over tropical oceans thus need not be tightly coupled, allowing for different phase variations which in turn create the complex patterns we find in Figure 3.

We note that our decomposition fails to capture the observed loops over Antarctica. Over much of Antarctica  $\mathcal{O}$  is small but clearly negative, whereas the sum of our decomposition would indicate a weakly positive loopiness (compare Figs. 3 and 5). Therefore seasonal covariance of lapse rates and humidity can be important in some regions, even though its influence is limited at a global scale.

## 5 Discussion

Our analysis up to now has shown that OLR loops are widespread, but what do these results imply about the mean shape of Earth’s seasonal  $\text{OLR}(T_s)$  relationship? After all, parts of the globe with large OLR loopiness might also experience a large seasonal cycle in OLR, such that the global mean of many local  $\text{OLR}-T_s$  relationships could still resemble a line. Similarly, our analysis focused on clear-sky data, but how are OLR loops affected by clouds?

To address these questions, Figure 6 shows  $\mathcal{O}$  normalized by the local annual range of OLR,  $\Delta\text{OLR}$ , using both clear-sky and all-sky data. If the  $\text{OLR}-T_s$  relationship was a straight line, then normalized loopiness would be zero; conversely, if the relationship was a perfect circle, then normalized loopiness would be  $\pi/4 \approx 80\%$  (it would be 100% for an  $\text{OLR}-T_s$  rectangle). Taking the global mean and magnitude of the data in Figure 6, we find  $\langle |\mathcal{O}|/\Delta\text{OLR} \rangle = 20\%$  for clear-sky data and  $\langle |\mathcal{O}|/\Delta\text{OLR} \rangle = 24\%$  for all-sky data (here, angle brackets denote an area-weighted global mean). The mean normalized OLR loopiness deviates from zero not only in the tropics, but also over ice-free extratropical oceans (Fig. 6). A line is therefore not a good fit for the typical shape of the seasonal  $\text{OLR}-T_s$  relationship at a given point on Earth.

Clouds largely preserve the spatial pattern of OLR loopiness (Fig. 6). In the Tropics and over most extratropical ocean areas, the annual OLR range as well as  $\mathcal{O}$  tend to be amplified by clouds, with a similar ratio for all-sky and clear-sky conditions. Over extratropical land masses and polar regions, clouds decrease the annual OLR range, but since  $\mathcal{O}$  is also small in these areas, this effect is hard to notice in the overall map of OLR loopiness (Fig. 6). To first order, the seasonal relationship between OLR and surface temperature appears robust to the presence of clouds.

Although this study focuses on the seasonal cycle, we speculate that OLR loops might also occur on longer time scales. Previous work showed that the clear-sky longwave feedback  $d\text{OLR}/dT_s$  from interannual variability shows significant scatter and differs from  $d\text{OLR}/dT_s$  on equilibrium time scales (Bony et al., 1995; Allan et al., 1999). However, the same studies also found that the linear fit between interannual clear-sky OLR and surface temperatures improves, and the inferred  $d\text{OLR}/dT_s$  becomes independent of time scale, if one removes

interannual variability in lapse rates and relative humidity. The same processes that give rise to seasonal OLR loops thus also seem to operate on yearly time scales.

Going to even longer variability, recent work found that the longwave feedback inferred from internal variability in CMIP5 Global Climate Models (GCMs) only approaches its equilibrium value on time scales longer than  $\sim 10$  years (Lutsko & Takahashi, 2018). A plausible explanation is that the spatial pattern of warming/cooling associated with internal variability differs from the warming pattern under CO<sub>2</sub> forcing (Andrews et al., 2018), and that warming in different parts of the world triggers distinct and non-local feedbacks (e.g., surface warming in the West Pacific can change tropospheric emission in the East Pacific without directly warming the surface in the East Pacific; Dong et al., 2019; Bloch-Johnson et al., 2020). Since these dynamics imply that local atmospheric changes under internal variability are not necessarily driven by changes in local surface temperature, the same dynamics that cause seasonal OLR loops might thus also occur on longer timescales, which would complicate inferences about Earth’s long-term feedbacks that are based on simple linear regression.

## 6 Conclusion

On seasonal time scales, the relationship between clear-sky OLR and surface temperature cannot typically be approximated as linear; instead it takes the form of complex curves or loops. Over extratropical continents OLR loopiness is close to zero. Over extratropical oceans OLR loops are caused by atmospheric warming that leads surface warming. By contrast, in the tropics OLR loops are caused by humidity variations; in monsoon regions humidity generally lags surface warming while more complex relationships arise over tropical oceans.

OLR loops imply that the seasonal cycle cannot be used as a direct analog for Earth’s response to global warming. Future work should consider whether similar behavior also persists on longer time scales.

### Acknowledgments

We thank two anonymous reviewers, Brian Rose for developing and maintaining CLIMLAB, and Nicholas Lutsko for helpful discussions.

ERA5 reanalysis data are from Copernicus Climate Change Service (C3S) (2017), ERA5: Fifth generation of ECMWF atmospheric reanalyses of the global climate. Copernicus Climate Change Service Climate Data Store (CDS), accessed 08-2020, <https://cds.climate.copernicus.eu/cdsapp#!/home>. CLIMLAB is publicly available at <https://doi.org/10.5281/zenodo.1226360>. CERES data were obtained from the NASA Langley Research Center Atmospheric Science Data Center, <https://ceres.larc.nasa.gov/data>. The code to reproduce our offline OLR calculations is available at: <https://doi.org/10.5281/zenodo.4766392>. Readers can find a high-resolution interactive version of the map of clear-sky OLR loopiness at <https://bdgrichards.github.io/OLR-Loop-Viewer>, with an archive available at <https://doi.org/10.5281/zenodo.4766402>.

## References

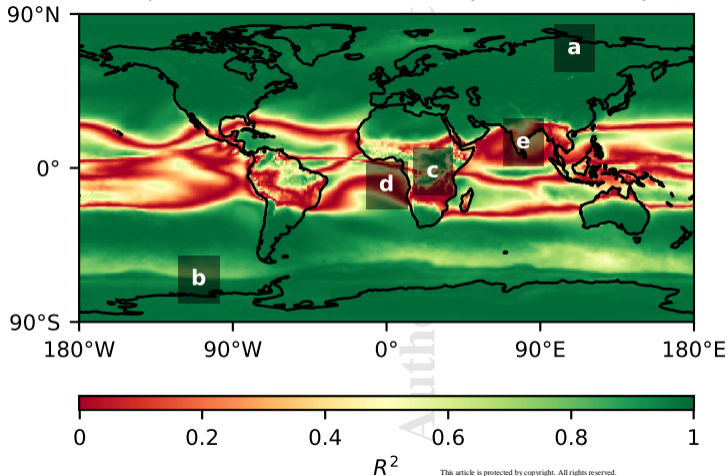
- Allan, R. P., Shine, K. P., Slingo, A., & Pamment, J. A. (1999). The dependence of clear-sky outgoing long-wave radiation on surface temperature and relative humidity. *Quarterly Journal of the Royal Meteorological Society*, *125*, 2103–2126.
- Andrews, T., Gregory, J. M., Paynter, D., Silvers, L. G., Zhou, C., Mauritsen, T., ... Titchner, H. (2018). Accounting for Changing Temperature Patterns Increases Historical Estimates of Climate Sensitivity. *Geophysical Research Letters*, *45*(16), 8490–8499. doi: 10.1029/2018GL078887



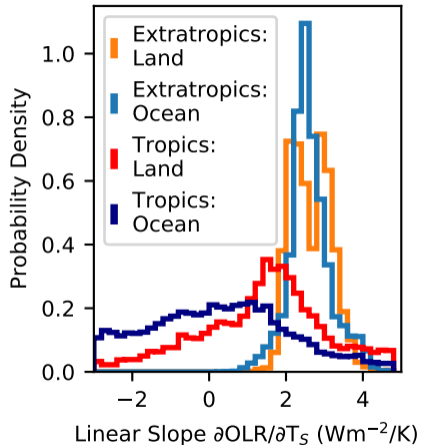
- Bloch-Johnson, J., Rugenstein, M., & Abbot, D. S. (2020, February). Spatial radiative feedbacks from internal variability using multiple regression. *Journal of Climate*. doi: 10.1175/JCLI-D-19-0396.1
- Bony, S., Duvel, J.-P., & Trent, H. L. (1995, July). Observed dependence of the water vapor and clear-sky greenhouse effect on sea surface temperature: Comparison with climate warming experiments. *Climate Dynamics*, 11(5), 307–320. doi: 10.1007/BF00211682
- Budyko, M. I. (1969, Jan 1.). The effect of solar radiation variations on the climate of the earth. *Tellus*, 21(5), 611–619. doi: 10.3402/tellusa.v21i5.10109
- Dessler, A. E. (2010, December). A Determination of the Cloud Feedback from Climate Variations over the Past Decade. *Science*, 330(6010), 1523–1527. doi: 10.1126/science.1192546
- Dong, Y., Proistosescu, C., Armour, K. C., & Battisti, D. S. (2019, September). Attributing Historical and Future Evolution of Radiative Feedbacks to Regional Warming Patterns using a Green’s Function Approach: The Preeminence of the Western Pacific. *Journal of Climate*, 32(17), 5471–5491. doi: 10.1175/JCLI-D-18-0843.1
- Forster. (2016, June). Inference of Climate Sensitivity from Analysis of Earth’s Energy Budget. *Annual Review of Earth and Planetary Sciences*, 44(1), 85–106. doi: 10.1146/annurev-earth-060614-105156
- Forster, & Gregory. (2006, January). The Climate Sensitivity and Its Components Diagnosed from Earth Radiation Budget Data. *Journal of Climate*, 19(1), 39–52. doi: 10.1175/JCLI3611.1
- Hartmann, D. L. (2016). *Global Physical Climatology* (Second Edition ed.). Newnes.
- Held, I. M., & Shell, K. M. (2012, February). Using Relative Humidity as a State Variable in Climate Feedback Analysis. *Journal of Climate*, 25(8), 2578–2582. doi: 10.1175/JCLI-D-11-00721.1
- Hersbach, H., Bell, B., Berrisford, P., Hirahara, S., Horányi, A., Muñoz-Sabater, J., ... Thépaut, J.-N. (2020). The ERA5 global reanalysis. *Quarterly Journal of the Royal Meteorological Society*, 146(730), 1999–2049. doi: 10.1002/qj.3803
- Huang, Y., & Ramaswamy, V. (2008). Observed and simulated seasonal co-variations of outgoing longwave radiation spectrum and surface temperature. *Geophysical Research Letters*, 35, L17803.
- Koll, D. D. B., & Cronin, T. W. (2018, Oct 9.). Earth’s outgoing longwave radiation linear due to h2o greenhouse effect. *Proceedings of the National Academy of Sciences of the United States of America*, 115(41), 10293–10298. doi: 10.1073/pnas.1809868115
- Loeb, N. G., Doelling, D. R., Wang, H., Su, W., Nguyen, C., Corbett, J. G., ... Kato, S. (2018, January). Clouds and the Earth’s Radiant Energy System (CERES) Energy Balanced and Filled (EBAF) Top-of-Atmosphere (TOA) Edition-4.0 Data Product. *Journal of Climate*, 31(2), 895–918. doi: 10.1175/JCLI-D-17-0208.1
- Lutsko, N. J., & Takahashi, K. (2018, April). What Can the Internal Variability of CMIP5 Models Tell Us About Their Climate Sensitivity? *Journal of Climate*. doi: 10.1175/JCLI-D-17-0736.1
- Mlawer, E. J., Taubman, S. J., Brown, P. D., Iacono, M. J., & Clough, S. A. (1997, July). Radiative transfer for inhomogeneous atmospheres: RRTM, a validated correlated-k model for the longwave. *Journal of Geophysical Research: Atmospheres*, 102(D14), 16663–16682. doi: 10.1029/97JD00237
- Murphy, D. M., Solomon, S., Portmann, R. W., Rosenlof, K. H., Forster, P. M., & Wong, T. (2009). An observationally based energy balance for the Earth since 1950. *Journal of Geophysical Research: Atmospheres*, 114(D17). doi: 10.1029/2009JD012105
- Pierrehumbert, R. T., & Roca, R. (1998, December). Evidence for control of Atlantic subtropical humidity by large scale advection. *Geophysical Research Let-*

- ters*, 25(24), 4537–4540. doi: 10.1029/1998GL900203
- Raval, A., Oort, A. H., & Ramaswamy, V. (1994). Observed dependence of outgoing longwave radiation on sea surface temperature and moisture. *Journal of Climate*, 7, 807–821.
- Rose, B. E. (2018, April). CLIMLAB: A Python toolkit for interactive, process-oriented climate modeling. *Journal of Open Source Software*, 3(24), 659. doi: 10.21105/joss.00659
- Schneider, E. K. (1996, December). *A Note On The Annual Cycle of Sea Surface Temperature at the Equator* (Tech. Rep. No. COLA Report 36). Calverton, MD 20705: Center for Ocean-Land-Atmosphere Studies.
- Zelinka, M. D., Myers, T. A., McCoy, D. T., Po-Chedley, S., Caldwell, P. M., Ceppi, P., . . . Taylor, K. E. (2020). Causes of higher climate sensitivity in cmip6 models. *Geophysical Research Letters*, 47(1). doi: 10.1029/2019GL085782
- Zhang, Y., Jeevanjee, N., & Fueglistaler, S. (2020). Linearity of Outgoing Longwave Radiation: From an Atmospheric Column to Global Climate Models. *Geophysical Research Letters*, 47(17), e2020GL089235. doi: 10.1029/2020GL089235

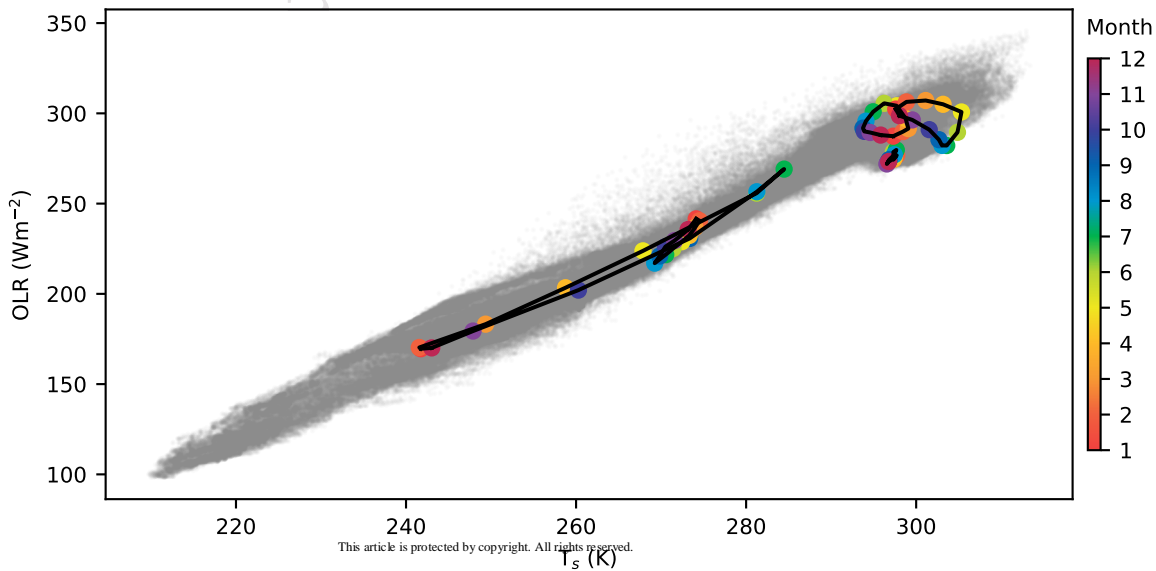
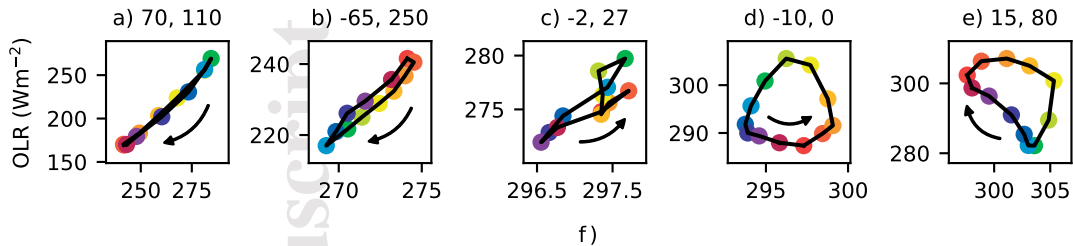
a) Map of  $R^2$  for Linear Fit of Monthly OLR to Monthly  $T_S$



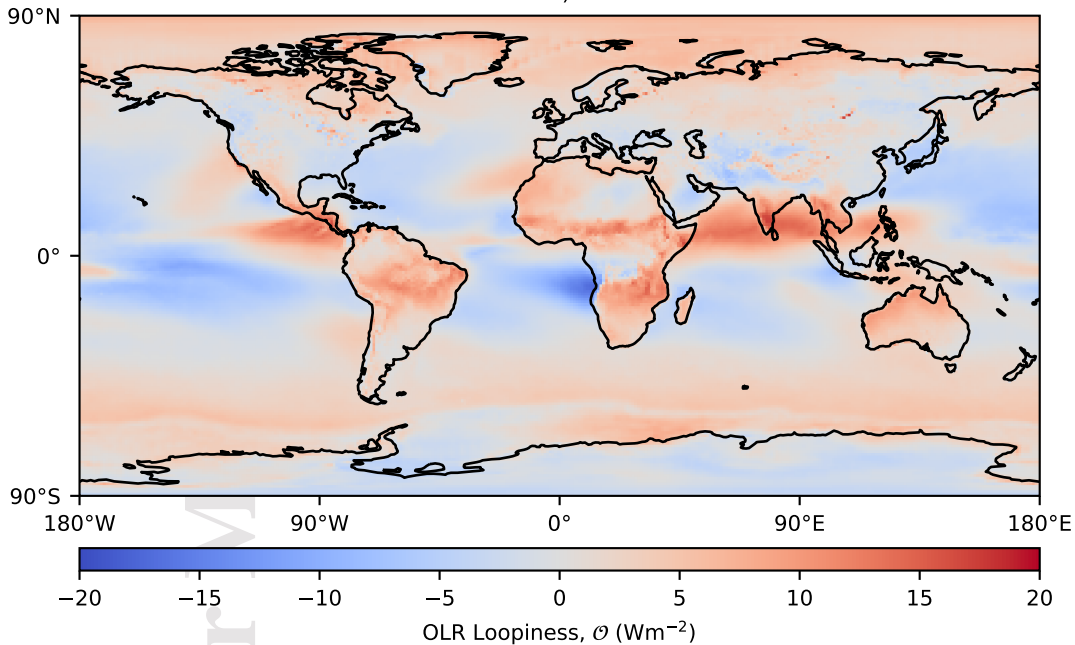
b) Histogram of Slope  $\partial\text{OLR}/\partial T_S$



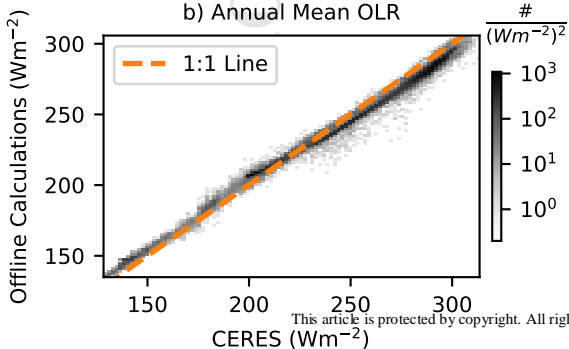
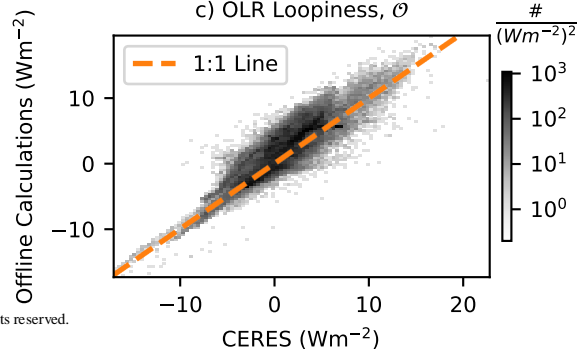
Latitude, Longitude

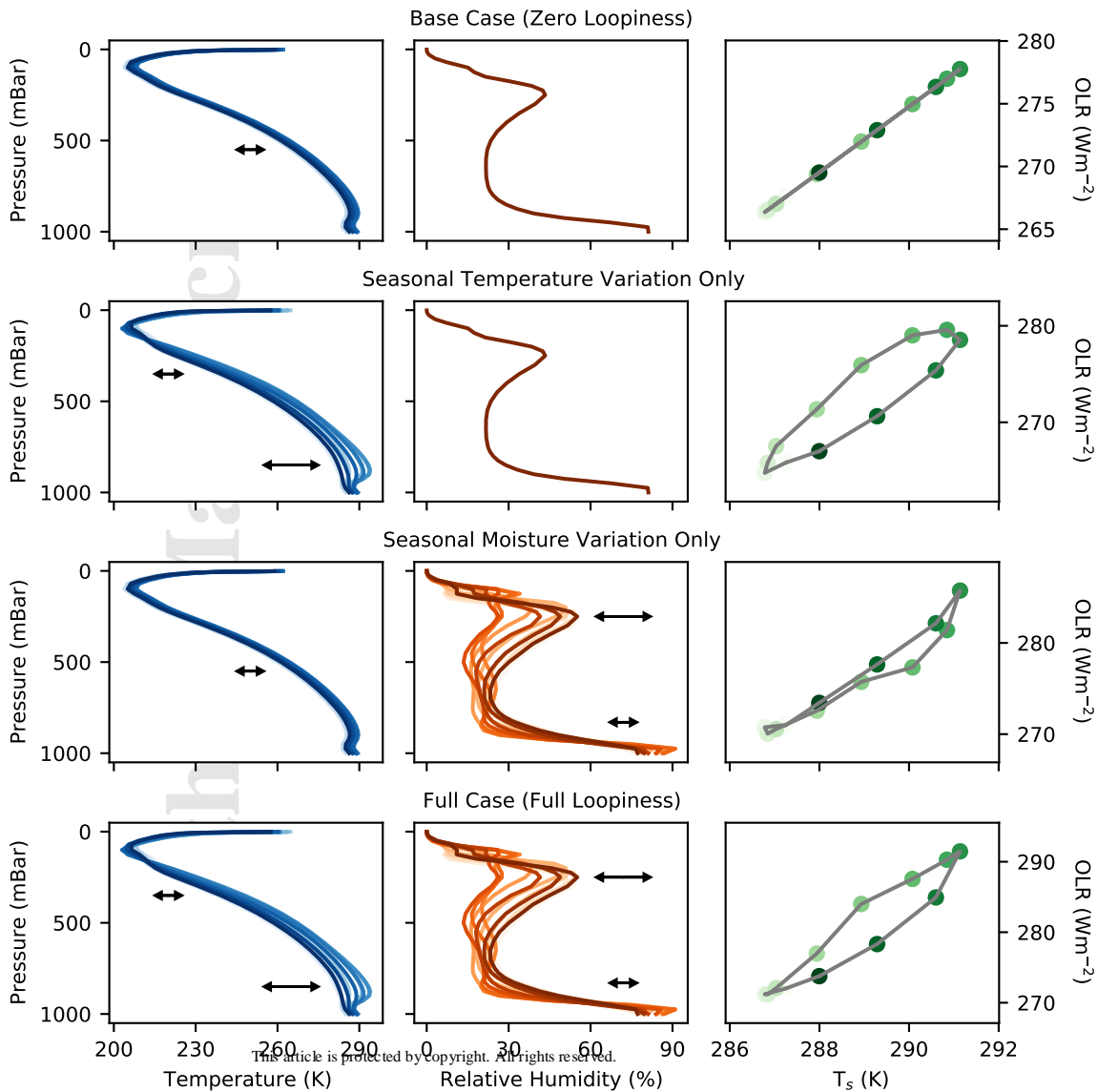


a)

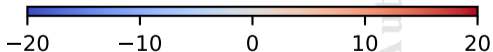
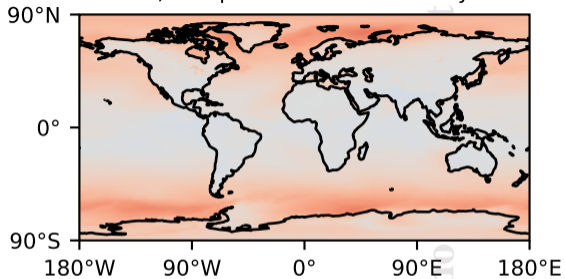


b) Annual Mean OLR

c) OLR Loopiness,  $\theta$ 

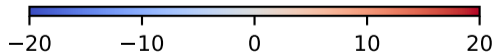
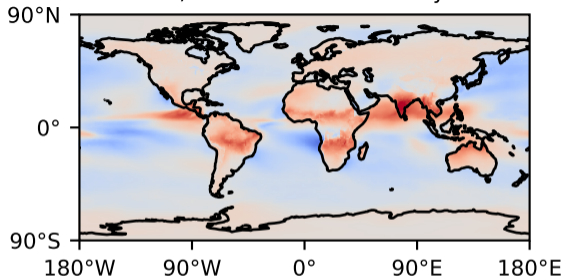


a) Temperature Variation Only



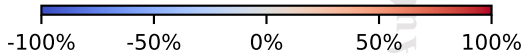
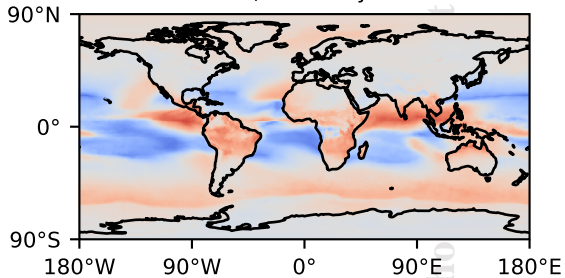
OLR Loopiness,  $\vartheta$  ( $\text{Wm}^{-2}$ )

b) Moisture Variation Only



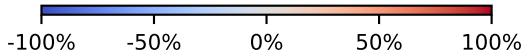
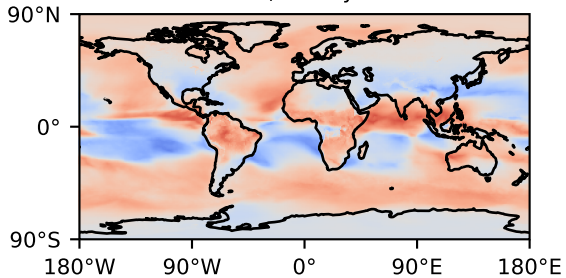
OLR Loopiness,  $\vartheta$  ( $\text{Wm}^{-2}$ )

a) Clear Sky



$\tau$  / OLR Range (%)

b) All Sky



$\tau$  / OLR Range (%)